Chapter 4 Surface Characteristics of Additively Manufactured Ti-6Al-4V Alloy

In this chapter, the effect of different grinding mediums on surface characterises of additively manufactured Ti-6Al-4V alloy is discussed. The surface was examined by scanning electron microscopy to evaluate the surface morphology. This chapter describes the grinding forces generated during finishing, surface roughness improvement, and temperature generated during grinding operation. AFM analysis was also carried out to evaluate the finished surface.

4.1 Results and Discussion

4.1.1 Grinding forces

During surface grinding, grinding forces are generated and they are affected by grinding parameters like depth of cut, table speed, and grinding environments, which can cause damage to the ground surface. The variation of tangential and normal grinding forces at different depth of cut (DOC) and table speeds in various grinding environments has been shown in Figure 4.1 (a) and (b), respectively. The grinding forces are generated by the shearing action of hard abrasive particles and grit sharpness [106].

The tangential forces show a variation from 5 to 35 N, 5 to 30 N, and 5 to 15 N under dry, wet, and cryogenic environments, respectively, when varying the DOC from 10 to 30 µm and table speed from 7 to 13 m/min. Similarly, the normal forces show a variation from 10 to 140 N, 9 to 105 N, and 8 to 70 N in dry, wet, and cryo environments, respectively. As the DOC increases, the grinding forces also increase in a dry environment.

In wet and cryo environments, the grinding forces decreased as compared to the dry environments [191]. The maximum grinding force is obtained at 30 μm DOC and 13 m/min table speed under a dry environment due to the combined effect of shearing and ploughing action. The wide variation of normal forces indicated the dominating nature of ploughing action in place of shearing action during the grinding process. The depth of grit increases with an increase in DOC, as a result of more penetration of grit into the ground surface, increases the grinding forces.

At high temperatures, the work materials get stuck with grits, reducing the sharpness of grits and hence increasing the grinding forces. As table speed increases, the grinding forces also increase because of the variation of uncut layer thickness. In wet grinding, lower grinding forces were observed by maintaining the sharpness of the grits of the grinding wheel. However, at high DOC, the cutting fluids could not be able to reach the grinding region due to the development of a boundary layer ahead of the grinding zone, hence increasing the grinding force.

Contrarily, during cryogenic grinding, the liquid nitrogen easily reaches the grinding zone and lowers the temperature that further reduces the grinding force as compared to other grinding environment conditions. During cryogenic grinding, the tangential forces were reduced by 57.14% as compared to dry and approx. 50% with respect to wet conditions, and the reduction in normal forces was approx. 50% with respect to dry and approx. 33.33% as compared to wet grinding for maximum DOC and table speed. An optimized delivery pressure of liquid nitrogen, as suggested by some researchers [115, 192] has shown an important effect in lowering the temperature around the grinding zone because liquid nitrogen penetrates the generated boundary layer formed by the high-speed grinding wheel.

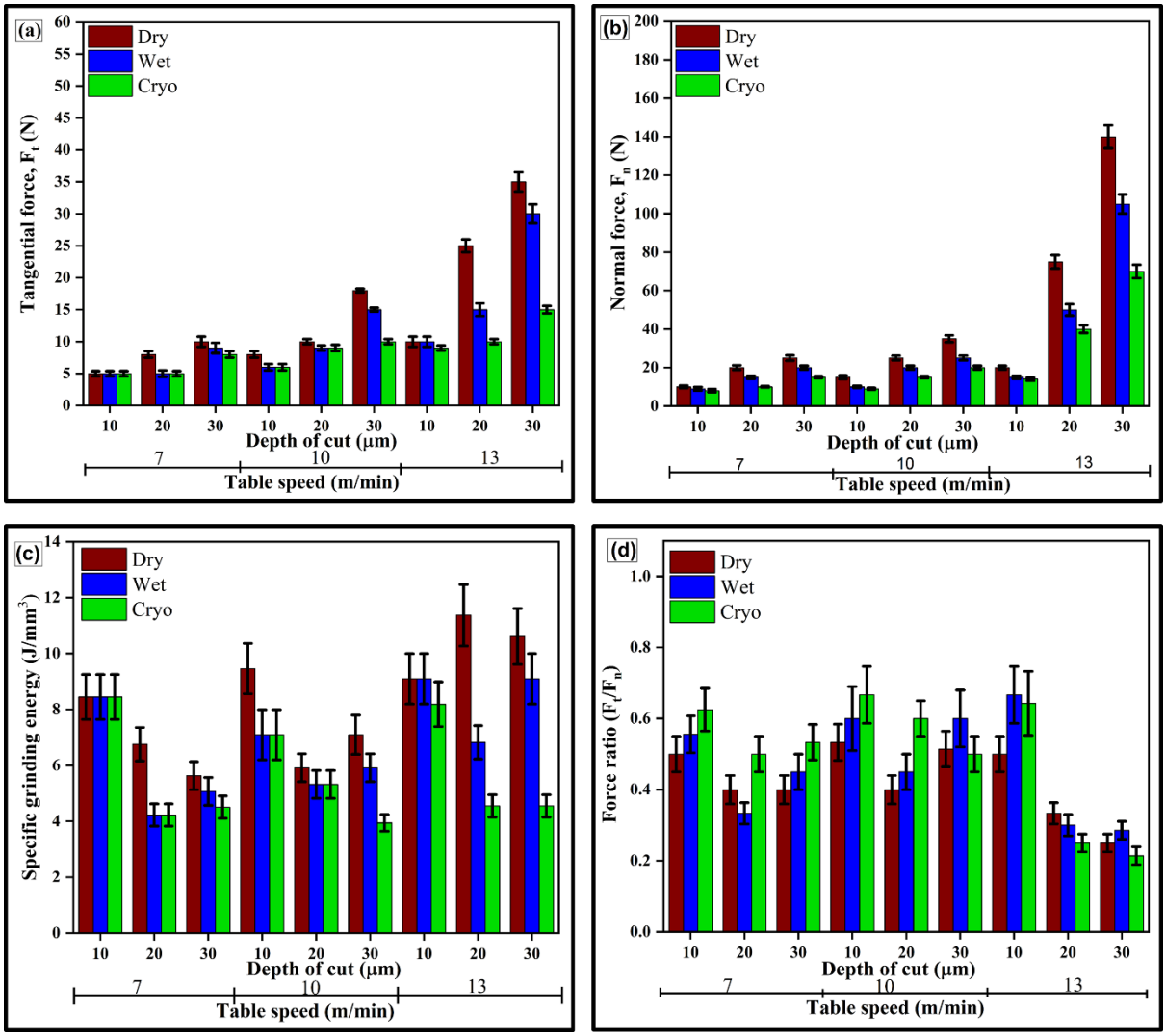

Figure 4.1 Variation in (a) tangential force, (b) normal force, (c) SGE, and (d) force ratio at different DOC and table speed under different environmental conditions

4.1.2 Specific grinding energy and force ratio

Figure 4.1 (c) illustrates the specific grinding energy (SGE) variation with respect to DOC and table speeds under different environmental conditions. The maximum SGE (11.37 J/mm^3) was obtained at 20 µm DOC and 13 m/min table speed in dry environment because of high grinding forces. This lower SGE indicates the process is more energy-efficient and environmentally benign. The maximum SGE in wet and cryogenic conditions was 9.10 J/mm^3 and 8.45 J/mm^3 respectively, which were 19.96% and 25.68%

less than that of under dry environment. The SGE decreased with an increase in DOC and table speed, except for increases in SGE observed at 13 m/min table speed. Due to pronounced shearing action caused by a reduction in ploughing and rubbing at higher DOC, a decrement in SGE was observed [193, 194].

In comparison with cryogenic environment, SGE was greater in wet conditions. Due to the low cutting fluid velocity in wet conditions, a hydrodynamic boundary layer forms surrounding the grinding region, increasing the rubbing action between the grinding wheel and workpiece and raising the temperature and grinding forces there. In comparison with cryogenic grinding, the consumption of SGE increases as the grinding forces increase in wet grinding. Cryogenic grinding reduces frictional forces between the grinding wheel and workpiece by injecting liquid nitrogen at a pressure that is optimal for the grinding zone and penetrates the hydrodynamic layer that was generated in wet grinding. The lower value of tangential forces during cryogenic grinding (Figure 4.1 (a)) reflects low energy utilization for removing the same volume of materials.

Another criterion that identifies the nature of interaction between the grinding wheel and workpiece is the effect of force ratio ($\frac{F_t}{F_n}$) on grinding performance. Figure 4.1 (d) represents the variation of force ratio compared to DOC and table speed in various environments. For the same table speed, the force ratio decreased with an increase in DOC because at high DOC, due to more contact length, a high shearing effect was observed by the sharp abrasive particles [107]. The lower force ratio (0.21) was observed for cryogenic grinding over dry and wet grinding at maximum DOC and table speed due to the generation of less heat in the grinding region [195]. The variation of force ratio was measured to be 0.25 to 0.53, 0.29 to 0.67, and 0.21 to 0.67 in dry, wet, and cryo environments, respectively.

4.1.3 Temperature

The development of the grinding zone temperature, which affects the workpiece's surface integrity, depends on a number of variables, including DOC, table speed, grit size, the velocity of the grinding wheel, and various environmental conditions. The temperature has been measured at the grinding zone (interface of grinding wheel and workpiece) which is maintained at a distance of 50 mm left from the tip of the cryo nozzle, as shown in Figure 2.3. At grinding zone, heat is generated due to contact between grinding wheel and workpiece. Out of these, the quantity of heat generated in the grinding region has been calculated using variables like DOC, table speed, and grinding conditions [196, 197] and the same is shown in Figure 4.2 under different grinding environment conditions. The minimum and maximum values of the grinding zone temperature are from 88°C to 383°C, 80°C to 252°C, and 39°C to 119°C in dry, wet, and cryo environments, respectively.

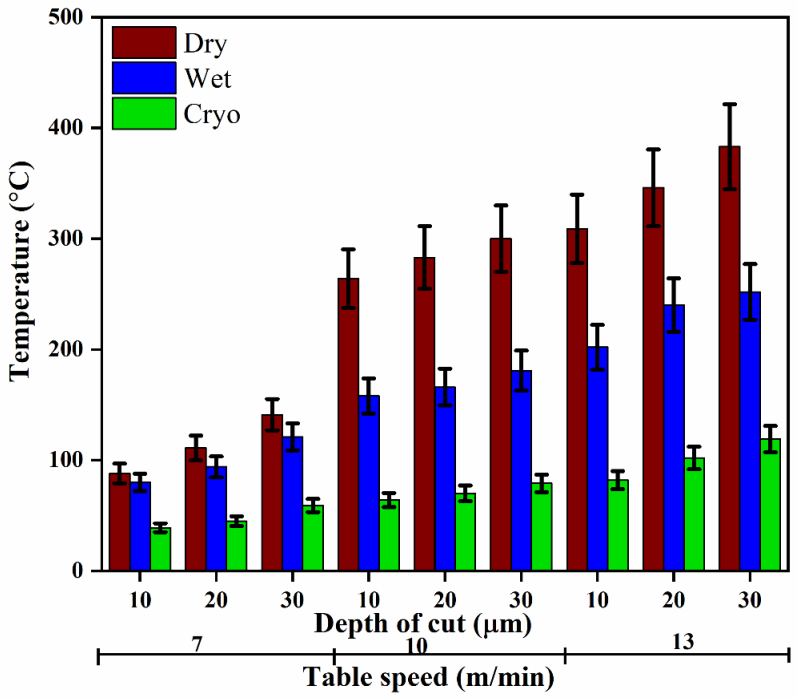

Figure 4.2 Variation in temperature under different environmental conditions

The grinding temperature rises as DOC and table speed increase due to friction developed in the grinding region [102], as shown in Figure 4.3. The maximum forces are generated in dry environment, raising the temperature in the grinding area. In the cryo environment, liquid nitrogen is uniformly sprayed and penetrates the hydrodynamic boundary layer at the interface region of grinding wheel and workpiece that absorbs the heat generated during grinding process. The chips generated during grinding carry away the heat developed in the grinding region [198].

The thermal camera images in various environments during the experiment are shown in Figure 4.3. The minimum and maximum values of the grinding zone temperature are from 88°C to 383°C, 80°C to 252°C, and 39°C to 119°C in dry, wet, and cryo environments, respectively. The temperature generated in cryo grinding was approx. 55% and 68.92% less than that of dry grinding at minimum and maximum DOC and table speed, respectively, also reported by other researchers [106, 113]. Again, the grinding temperature was about 51.25% and 52.78% less than wet grinding at minimum and maximum DOC and table speed, respectively.

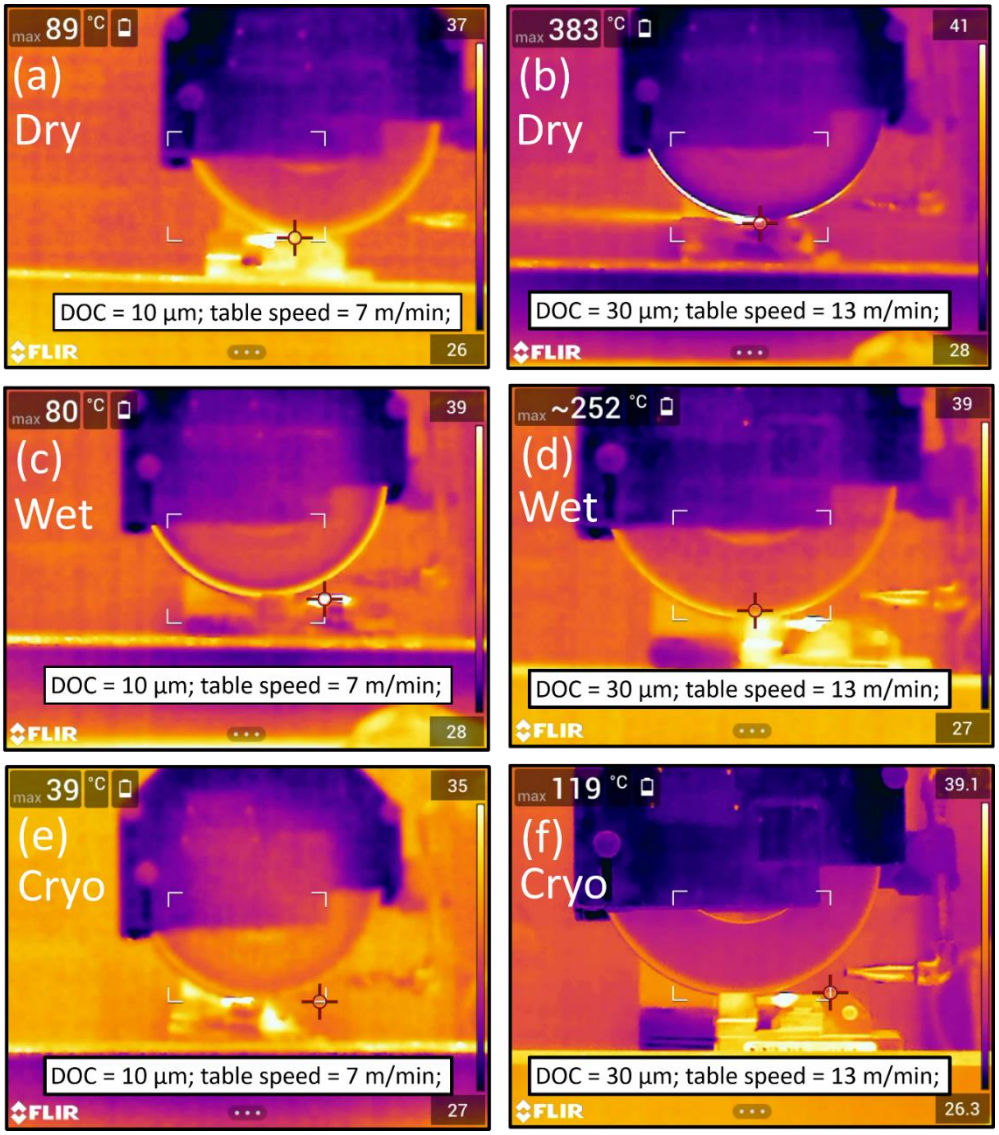

Figure 4.3 Thermal camera images captured (a, b) dry grinding; (c, d) wet grinding, and (e, f) cryogenic grinding at different DOC, and table speed under different environmental conditions

4.1.4 Surface roughness of finished L-PBF Ti-6Al-4V alloy

Figure 4.4 shows the average surface roughness (R_a) of L-PBF Ti-6Al-4V material at various DOC, table speeds, and different grinding environment conditions. After the L-PBF process, the initial R_a value of the as-fabricated Ti-6Al-4V samples were observed to be between 3.89-5.94 µm. After the grinding operation, the R_a value has been improved by using different grinding environments at different DOC and table speeds. The R_a

values in different grinding environments have been compared. As the DOC and table speed increase, the R_a value increases in all environments due to the high undeformed chip thickness at higher DOC. In cryogenic grinding, at lower DOC and table speed, lower surface roughness was measured as 0.259 µm.

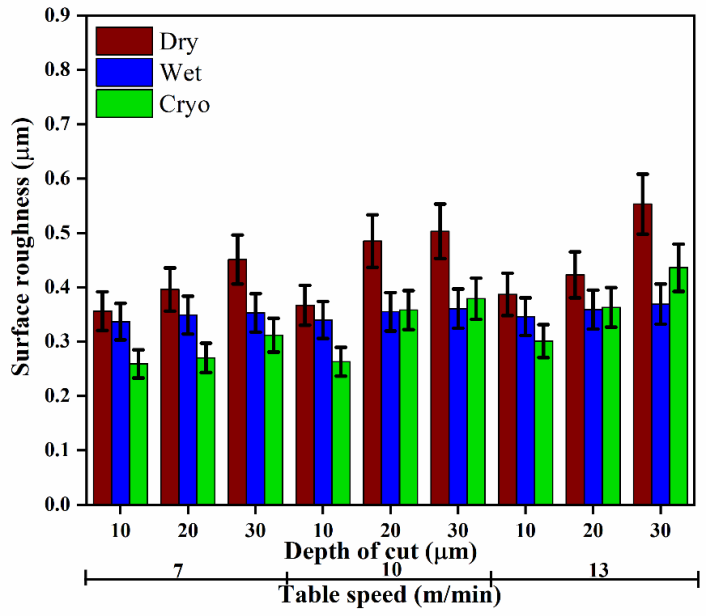

Figure 4.4 Surface roughness variation of grinded AM samples under various grinding environment conditions

At higher DOC, the penetration of the grinding wheel on the work-piece surface increases, which reduces the grit sharpness and that resulted in increased surface roughness. In cryogenic grinding, the R_a value was decreased by 27.25% and 23.15% in comparison to dry and wet conditions respectively. In general, the higher the grit sharpness, the lower the surface roughness, implying that grit sharpness is critical in improving the surface quality of L-PBF Ti-6Al-4V alloy [199]. R_a value was lowered from 5.94 µm to 0.356 µm, 0.337 µm, and 0.259 µm under dry, wet, and cryo environments, respectively.

The minimum R_a value was measured in cryo conditions because the liquid nitrogen was sprayed in the grinding region, which reduces the grinding zone temperature and therefore reduces the surface roughness. The sharpness of the grit is retained throughout the grinding operation due to the reduction in grinding zone temperature.

There is no direct relationship between the generating temperature and the surface roughness parameter, but there is an indirect effect of the grinding zone temperature on the surface roughness of the workpiece. From the literature survey, we found that as the generated temperature increases, the surface roughness of the workpiece also increases, which is detrimental to the surface integrity of the finished sample in terms of changes in microhardness, oxidation on the top surface, and induction of tensile residual stresses [196]. Therefore, lower grinding temperature results in better surface finishes.

4.1.5 Surface roughness of finished AM and conventional samples

The average surface roughness (R_a) was evaluated measuring the roughness of the finished AM and conventional Ti-6Al-4V samples. The initial parameter, R_a of conventionally processed and the L-PBF components in heat-treated conditions was found to be 3.74 ± 1.18 µm and 8.95 ± 1.58 µm, respectively. After finishing operation, the average surface roughness was improved under different conditions, especially by cryogenic grinding.

As shown in Figure 4.5, parameter, R_a increased when the DOC and table feed increased under various grinding conditions because of large undeformed chip thickness. Increase in DOC causes deeper penetration of the grinding wheel and deeper into the workpiece surface, and diminishes in the sharpness of the abrasive grit increased surface roughness. If table feed is increased, the grinding wheel is being forced to remove more material in a shorter time. This causes the wheel to become dull more quickly and

generate heat between the wheel and workpiece. This heat causes the workpiece to expand, which increases surface roughness.

In general, surface roughness decreases as grit sharpness increases, suggesting that the sharpness of abrasive grit is essential for enhancing the surface characteristics of components [199]. Lower surface roughness was observed in cryogenic grinding at DOC of 20 µm and table feed of 07 m/min, and it was 0.259 µm for AM and 0.353 µm for conventionally processed sample. At DOC of 20 µm and table feed of 07 m/min, it was 0.356 µm for AM and 0.505 µm for conventionally processed sample in dry grinding and 0.337 µm for AM and 0.498 µm for conventionally processed sample in moist grinding.

The average surface roughness in cryogenic grinding was reduced by 27.25% and 23.15% for AM and 30.08% and 29.13% for conventional samples, compared to dry and moist conditions, respectively. In cryogenic grinding, liquid nitrogen was injected in the grinding area which lowered the temperature in the grinding area, as a result, surface roughness reduced. The drop in the temperature of the grinding zone allows the grit to maintain its sharpness throughout the grinding process. The grinding temperature is not directly correlated with the surface finish of the workpiece. According the literature review, as the temperature rises, the surface finish decreases because of decrease in hardness and increase of oxidation of the grinded surface [196]. Therefore, superior surface finishes are obtained at lower grinding temperatures.

The surface finish is affected by various factors such as depth of cut, table feed, and type of coolant used. In AM samples, wet grinding produced a better surface finish compared to cryogenic grinding at higher depth of cut and table feed. Cryogenic grinding uses liquid nitrogen as a coolant to cool the sample and the grinding wheel, which causes thermal stresses and cracking of the samples, and also causes rapid wear of the grinding

wheel, resulting in a less uniform grinding action and a rougher surface finish at higher depth of cut and table feed.

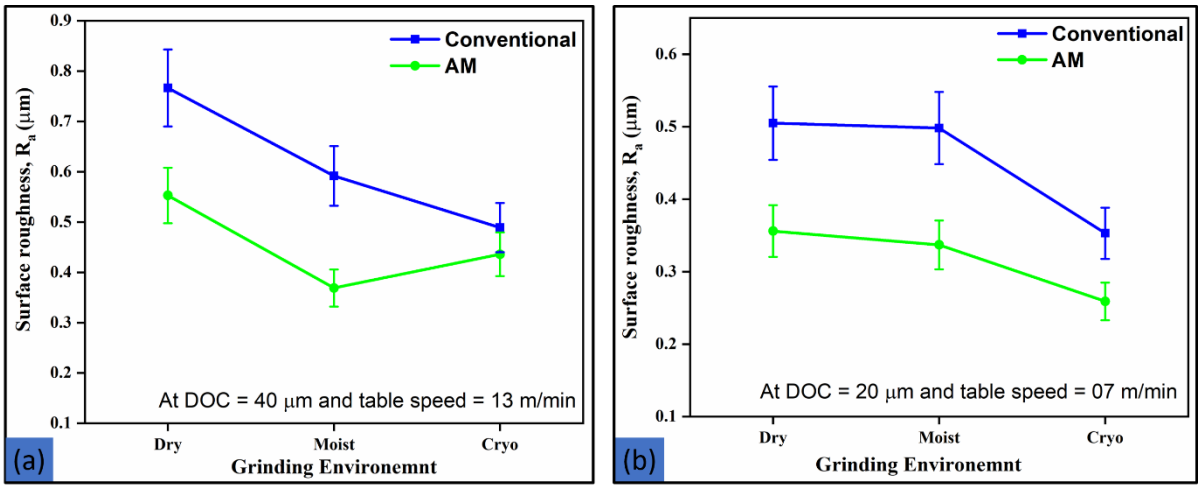

Figure 4.5 Surface roughness of finished AM and conventionally processed components: (a) at DOC of 40 μm and table feed of 13 m/min and (b) at DOC of 20 μm and table feed of 07 m/min

4.1.6 Surface morphology of finished L-PBF Ti-6Al-4V alloy

Figure 4.6 represents the SEM micrograph of the ground surface at maximum DOC under different grinding conditions. The surface quality of ground surfaces plays an important role with respect to applications. During dry grinding, poor surface quality has been observed (Figure 4.6 (a) and (b)) because of the presence of the deep grooves and eventually deposited layer on the grinded surface in the absence of coolant. The temperature during dry grinding was maximum and hence it increased the adhesion capability of the work material, thereby the chance of redeposition of layer. In wet grinding, the surface quality of ground surface was comparatively better (Figure 4.6 (c) and (d)) in respect of dry grinding, but at some places, deep grooves were observed due to incomplete penetration of coolant or restricted performance of coolant around the grinding zone. Figure 4.6 (e) and (f) show SEM micrographs of the ground surface under

cryogenic conditions. Cryo grinding produced a better surface quality than dry and wet grinding at lower DOC, but at higher DOC, some redeposited layers were observed, as shown in Figure 4.6 (f).

For further confirmation, Figure 4.7 represents the atomic force micrograph to analyse the 3D surface characteristics of grinded surfaces in different environments. The ground samples were scanned over a 30 x 30 µm area, as mentioned in Figure 4.7 (a, c and e). Again, the same samples were scanned over a 70 x 70 µm area (Figure 4.7 (b, d, and f)) to check the surface topography and surface roughness at the nano level. For a 70 x 70 µm scan area, the average surface roughness (S_a) values were measured as 229 nm, 164.3 nm, and 137 nm and the root means square surface roughness (S_q) values were 299, 204, and 187 nm in dry, wet, and cryo environments, respectively. However, for a 30 x 30 µm scan area, the S_a values were measured as 201.15, 128.3, and 118.4 nm and the S_q values were 255.5, 159.2, and 145.3 nm in dry, wet, and cryo environments, respectively.

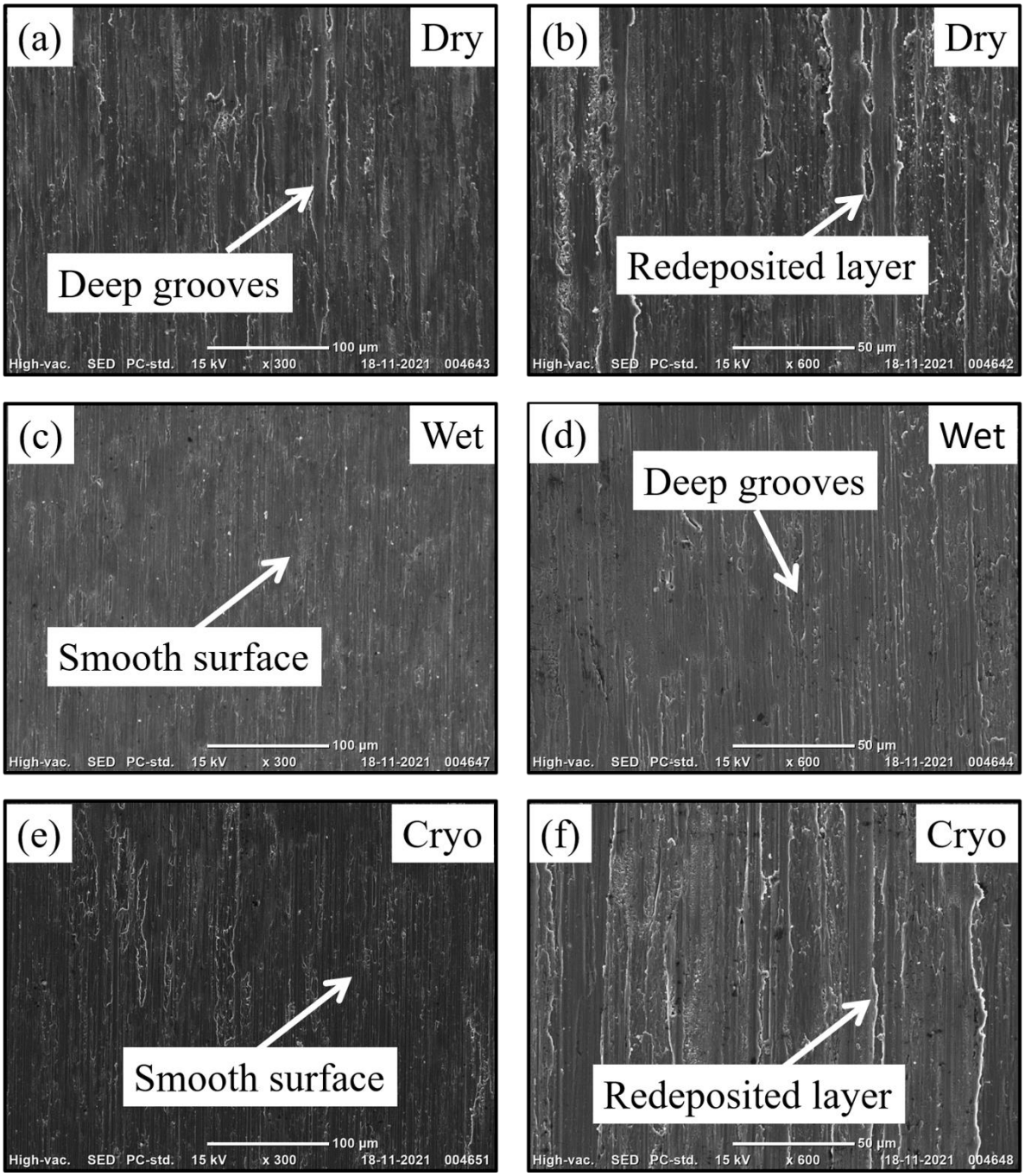

Figure 4.6 SEM micrographs of grinded surfaces for different grinding environment conditions: (a, b) dry, (c, d) wet, and (e, f) cryogenic conditions. (a), (c), and (e) at lower DOC and (b), (d), and (f) at higher DOC

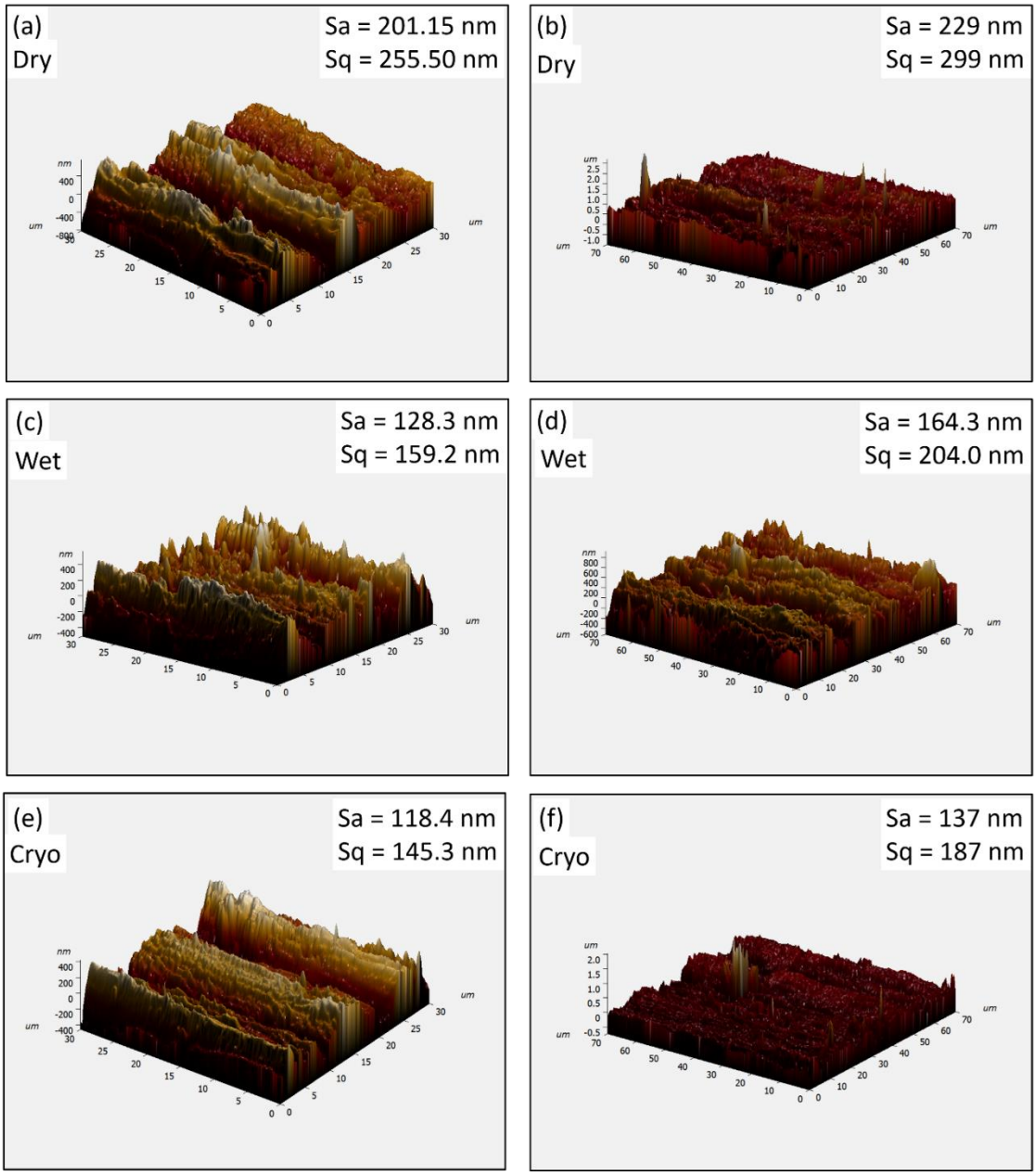

Figure 4.7 Atomic force microscopy micrograph of finished samples in: (a, b) dry, (c, d) wet, and (e, f) cryogenic conditions

The S_a value in cryo grinding was nearly half of dry grinding, which may be the reason for sufficient cooling in the grinding zone. After the first pass of dry grinding, the micro-chips stuck to the grinded surface, and these micro-chips were crushed over the grinded surface and deposited over the grinding wheel during the second pass, as a result of this, deep notches appeared on the grinded surfaces, as shown in Figure 4.7 (a).

The use of coolant during wet and cryogenic grinding allows for the removal of grinding debris from the ground surface and, due to this, S_a and S_q values were lower than that during dry grinding. In wet grinding, approx. 90% water was mixed with synthetic oil to increase the removal of heat from the grinding region and enhance cooling during the grinding process. In cryo grinding, lower average surface roughness was observed with respect to dry and wet grindings because of effective cooling in the grinding zone [112, 113].

4.1.7 Surface morphology of finished AM and conventional samples

Figure 4.8 presents SEM micrographs of finished surfaces of AM and conventional samples at DOC of 40 µm and table feed of 13 m/min. The surface quality of the finished components plays a crucial role in their applications. Poor surface quality has been seen from dry grinding (Figure 4.8 (a_1) and (a_2)) due to deep grooves and redeposited layer, in the absence of coolant. A layer of dislodged material gets redeposited because of increase in adhesion ability of workpiece in dry grinding condition.

In moist grinding, redeposited layers and deep groves were seen at some locations because of insufficient coolant penetration around the grinding region but the surface quality of finished samples was somewhat better than that in dry grinding (Figure 4.8 (b_1) and (b_2)). SEM image of the finished surface under cryogenic grinding, is shown in Figure 4.8 (c_1) and (c_2). At DOC of 40 µm and table feed of 13 m/min, cryogenic grinding generated a surface quality that was superior to dry and moist grinding. The surface characteristics of finished AM samples were better than those of finished conventional samples. Since the conventional samples are more ductile than the AM samples, their surface is rougher than that of AM samples.

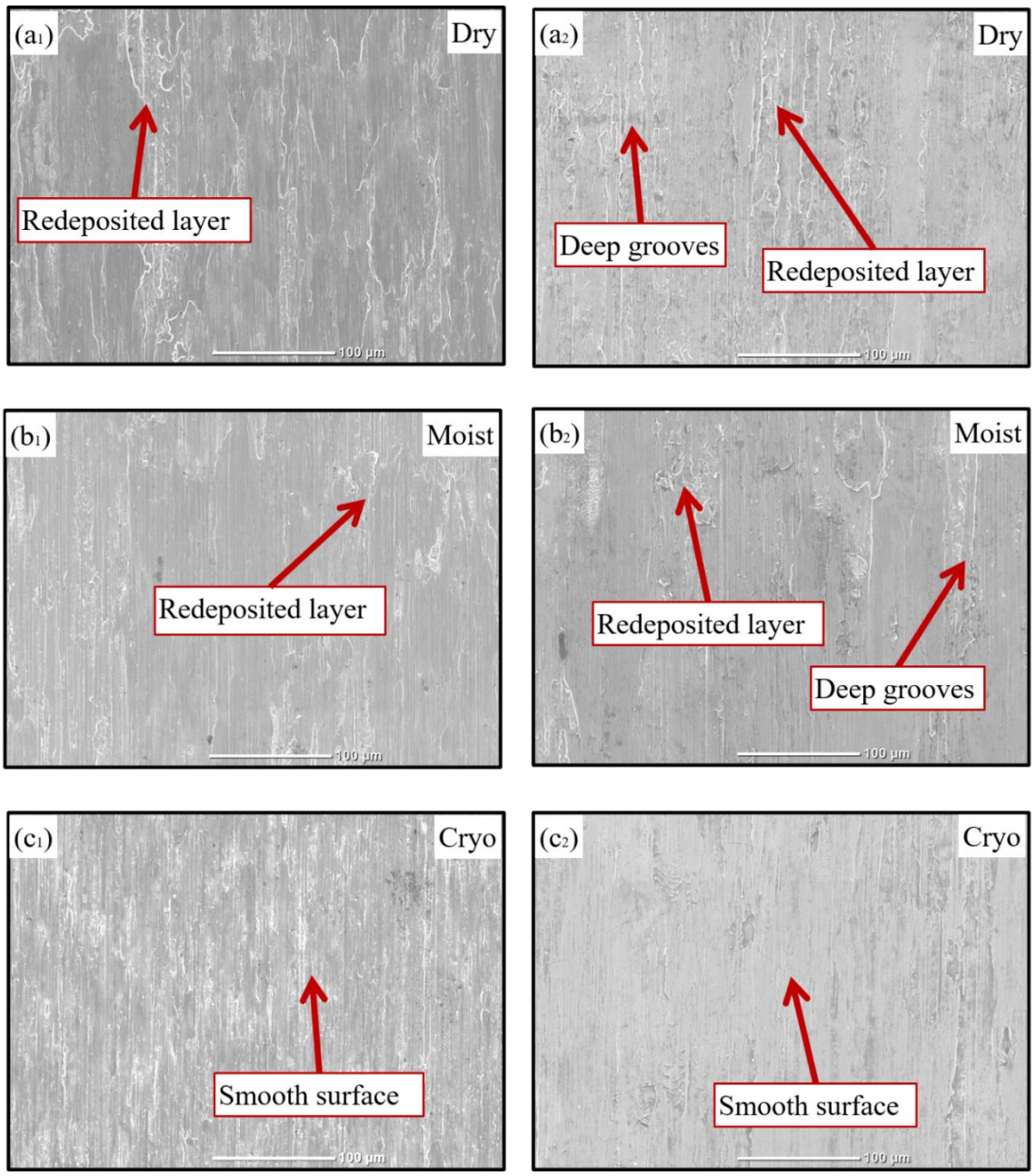

Figure 4.8 SEM micrographs of finished AM and conventionally processed samples at DOC of 40 µm and table feed of 13 m/min: (a) dry, (b) moist, and (c) cryogenic conditions. Subscript 1 is for AM and 2 for conventionally manufactured samples

For further confirmation, Figure 4.9 presents the trend of average surface roughness (S_a) of finished AM and conventional samples obtained from atomic force microscopy (AFM) at DOC of 40, 20 µm and table feeds of 07, 13 m/min in various conditions to evaluate the 3D surface morphology. At DOC of 20 µm and table feed of 07 m/min, both AM and

conventional finished samples exhibit almost same surface roughness (Figure 4.9 (b)). But at DOC of 40 µm and table feed of 13 m/min, higher surface roughness was found in the finished conventional samples in comparison with the finished AM samples (Figure 4.9 (a)) because of more ploughing action.

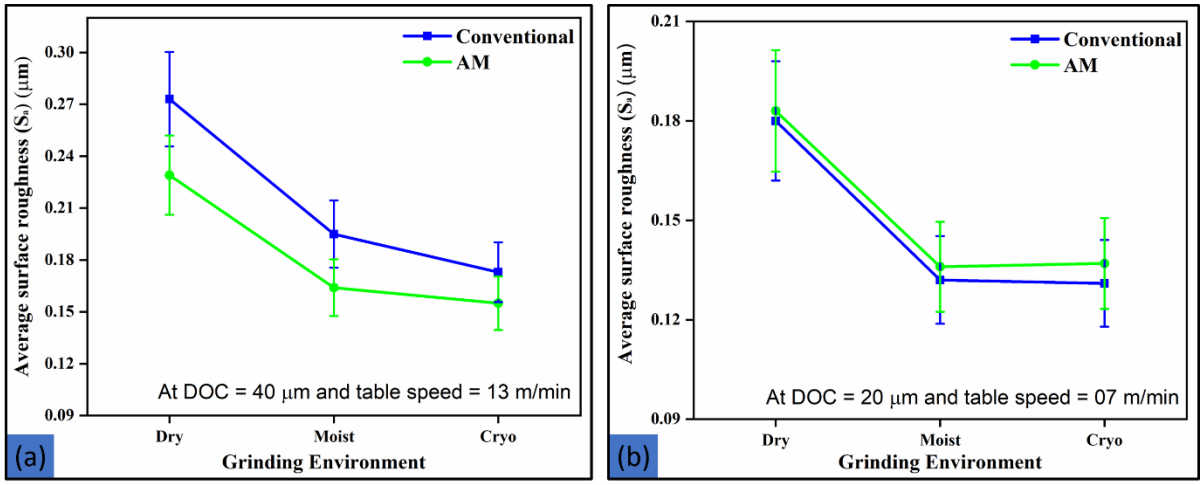

Figure 4.9 Average surface roughness obtained from atomic force microscopy: (a) at DOC of 40 µm and table feed of 13 m/min and (b) at DOC of 20 µm and table feed of 07 m/min

Figure 4.10 presents AFM images of finished AM and conventional samples at DOC of 40 µm and table feed of 13 m/min. Area of 70 x 70 μm^2 was examined for finished samples. From this figure, it may be observed that the finished conventional samples (Figure 4.10 (a_2), (b_2), and (c_2)) had larger peaks than the finished AM samples (Figure 4.10 (a_1), (b_1), and (c_1)). The parameter, S_a was observed as 229 nm, 164 nm, and 155 nm for the AM and 273 nm, 195 nm, and 173 nm for the conventional samples in dry, moist, and cryogenic conditions, respectively.

In dry grinding, micro-sized chips formed over the finished area during the first pass and then deposited on the abrasive wheel during another pass, because of this, deep grooves were observed on the finished surface of AM samples. This phenomenon is more

noticeable in finished conventional samples because of their high ductility. To enhance surface quality of the samples, moist grinding was performed but effective cooling in cryogenic grinding resulted in lower surface roughness, compared to dry and moist grinding as observed also earlier [112, 113].

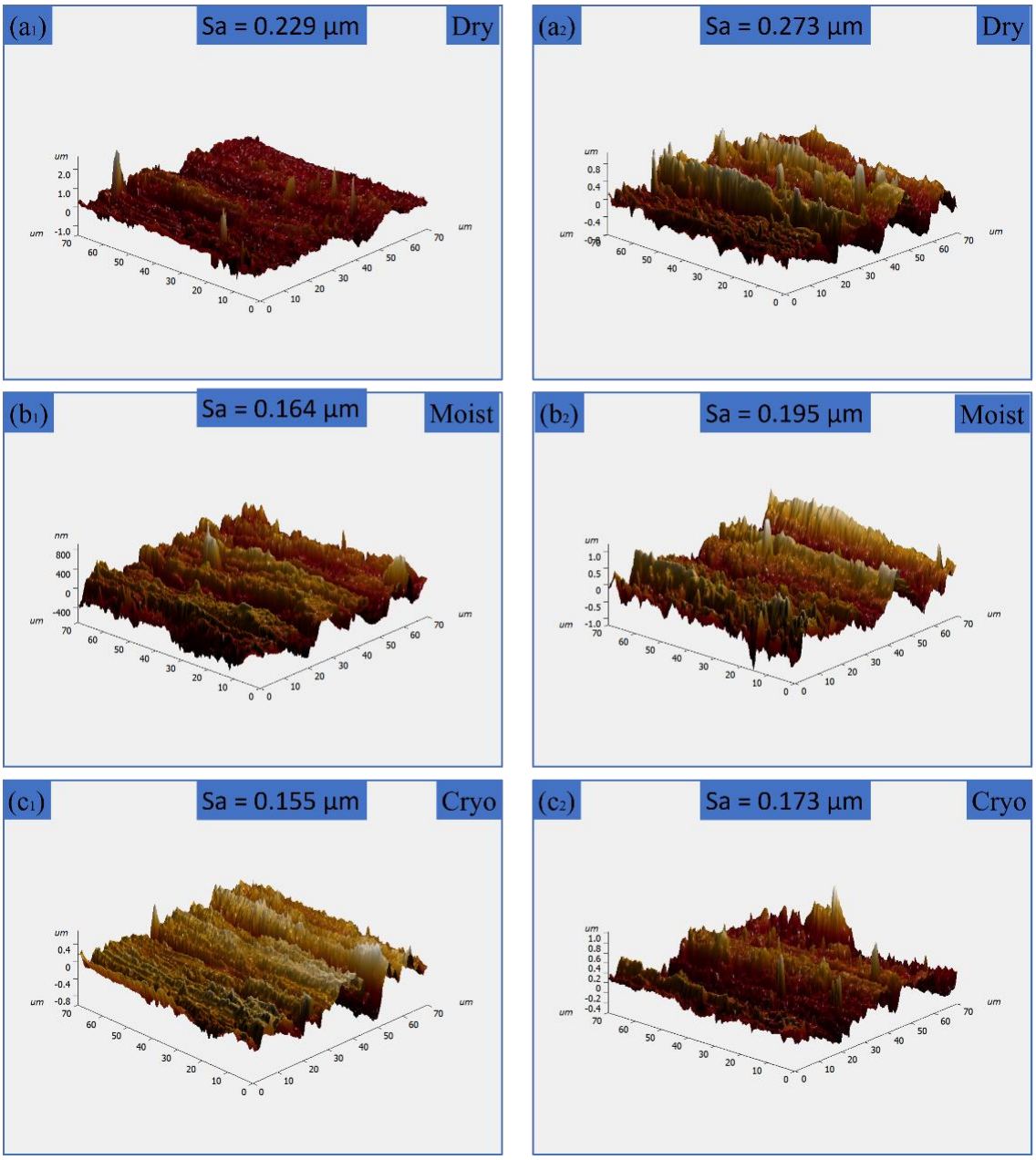

Figure 4.10 AFM images of finished AM and conventionally processed samples at DOC of 40 µm and table feed of 13 m/min: (a) dry, (b) moist, and (c) cryogenic conditions. Subscript 1 is for AM and 2 for conventionally manufactured samples

Suggested values of DOC and table feed for conventionally fabricated Ti-6Al-4V samples were used for finishing of the AM samples. The positive surface roughness results highlight that the above set of DOC and table feed can be used even when AM Ti-6Al-4V specimens are subjected to finishing operations, to enhance the surface quality.

4.1.8 Microhardness of finished L-PBF Ti-6Al-4V alloy

Figure 4.11 represents the microhardness of L-PBF Ti-6Al-4V alloy after finishing by the grinding process at different DOC and table speeds under different grinding conditions. The initial microhardness of the AM Ti-6Al-4V alloy was 427.8 ± 20 $HV_{0.2}$. The microhardness varied from 432.81 to 488 $HV_{0.2}$, 449.39 to 488.71 $HV_{0.2}$, and 450.17 to 502.85 $HV_{0.2}$ at a minimum and maximum DOC and table speed in different environments respectively.

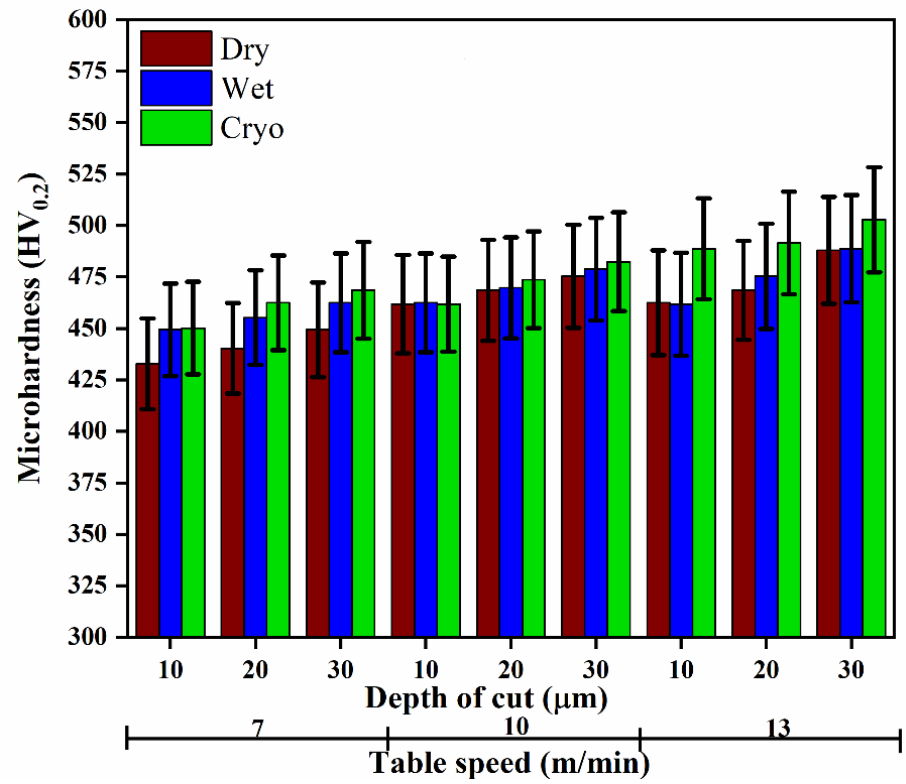

Figure 4.11 Variation of microhardness in different environment conditions

As DOC increases, the microhardness also increases because of increased tangential and normal forces during dry grinding. The same trend was observed with increasing the table speed. Dry grinding produces lower microhardness than wet or cryogenic environments due to faster heating and slower cooling of grinded surfaces. In wet grinding, similar results were observed due to the development of a boundary layer surrounding the grinding area, with a slight change in microhardness. Furthermore, effective cooling of the workpiece has occurred during cryogenic grinding, lowering the temperature and hardening the material. The frozen grinding region is formed in cryo grinding due to the spray of liquid nitrogen, which increases the microhardness of the material [196, 200].

4.1.9 Microhardness of finished AM and conventional samples

The microhardness measurements have also been performed on each finished sample at various DOC and table feeds in various grinding conditions and three measurements were taken at same place to check the reproducibility of finished samples. Figure 4.12 (a) and (b) present the maximum microhardness for the AM and conventional samples at low and high DOC and table feed, respectively. It is clear that the microstructure and microhardness of additively manufactured samples were different in comparison with that of the conventionally fabricated specimens. The hardness of AM samples was measured to be 17.81 % higher than that of the conventional samples. The trend of the results shows that the samples finished in cryogenic condition have the highest microhardness for the specimens produced by both the processes.

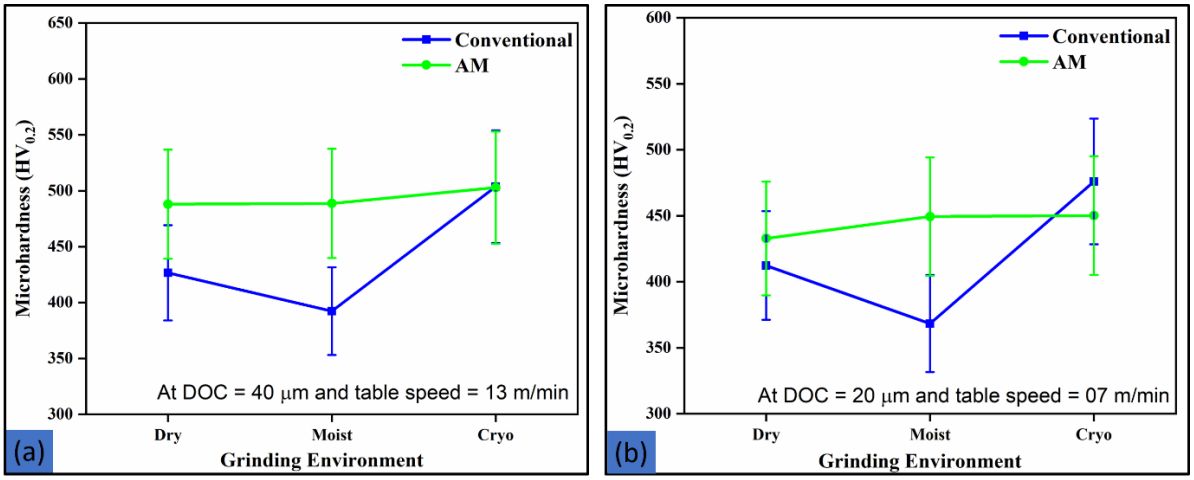

Figure 4.12 Maximum microhardness for AM and conventional components at (a) DOC of 40 µm and table feed of 13 m/min and (b) DOC of 20 µm and table feed of 07 m/min under different grinding conditions

4.1.10 Bearing area curve of finished AM and conventional samples

Figure 4.13 presents the variation of surface height of finished samples at DOC of 40 µm and table feed of 13 m/min in dry, moist, and cryogenic conditions. The difference between upper (Sr_1) and lower (Sr_2) material ratio was measured in the bearing area curve for better understanding of the surface topography. Figure 4.13 (a) and (b) show the trends of surface height with respect to bearing area percentage for finished AM and conventional samples, respectively.

According to this, the differences in upper and lower ratio were 76.73%, 79.35%, and 79.82% for finished AM and 73.95%, 81.69%, and 82.61% for finished conventional samples in dry, moist, and cryogenic conditions, respectively. In dry grinding, larger sharp points in the surface profile (Figure 4.10 (a_1) and (b_1)) of the material being finished are a result of a lower bearing area ratio, which leads to poor bearing properties.

The wide bearing area curve and high bearing ratio indicate the development of an excellent antifriction ground surface in the case of cryogenic environment. Additionally, the surface bearing index was lower under dry environment in comparison with moist and cryogenic conditions. The surface bearing indexes were 0.135 µm, 0.332 µm, and 0.482 µm for the finished AM and 0.300 µm, 0.411 µm, and 0.493 µm for the finished conventional sample under dry, moist, and cryogenic conditions, respectively. During cryogenic grinding, the sharpness of abrasive grit increased which influenced the topographic features of the finished samples, resulting in an increased surface bearing index.

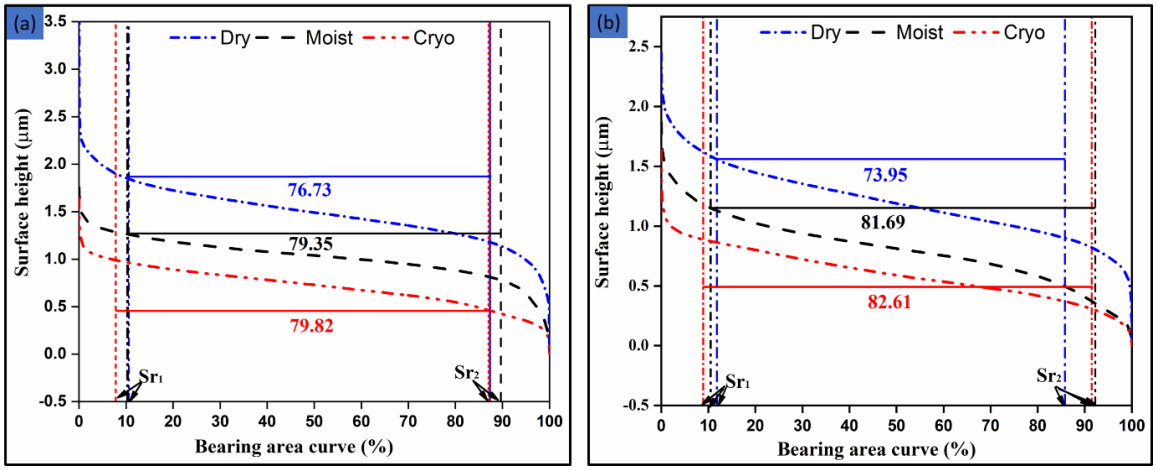

Figure 4.13 Surface height variation of finished (a) AM and (b) conventional samples at DOC of 40 µm and table feed of 13 m/min in dry, moist and cryogenic conditions

4.1.11 X-ray diffraction analysis of finished AM and conventional samples under different conditions

XRD analysis of the finished AM and conventional samples has been evaluated to visualize the effect of DOC and table feeds on the change in peaks, as shown in Figure 4.14. The XRD results of the finished samples indicated flattening of the peaks and the

peaks of the β phase were shown to be smaller than those of the as-fabricated samples because of the finishing operations. These findings are in agreement with those of other researchers [201, 202]. The modification in the XRD results like broadening of peaks was caused due to plastic deformation during finishing operations. Figure 4.14 (a_1, b_1, and c_1) and (a_2, b_2, and c_2) show the effect of DOC, table feeds, and various grinding conditions on the XRD patterns of finished additively manufactured and conventionally manufactured samples, respectively.

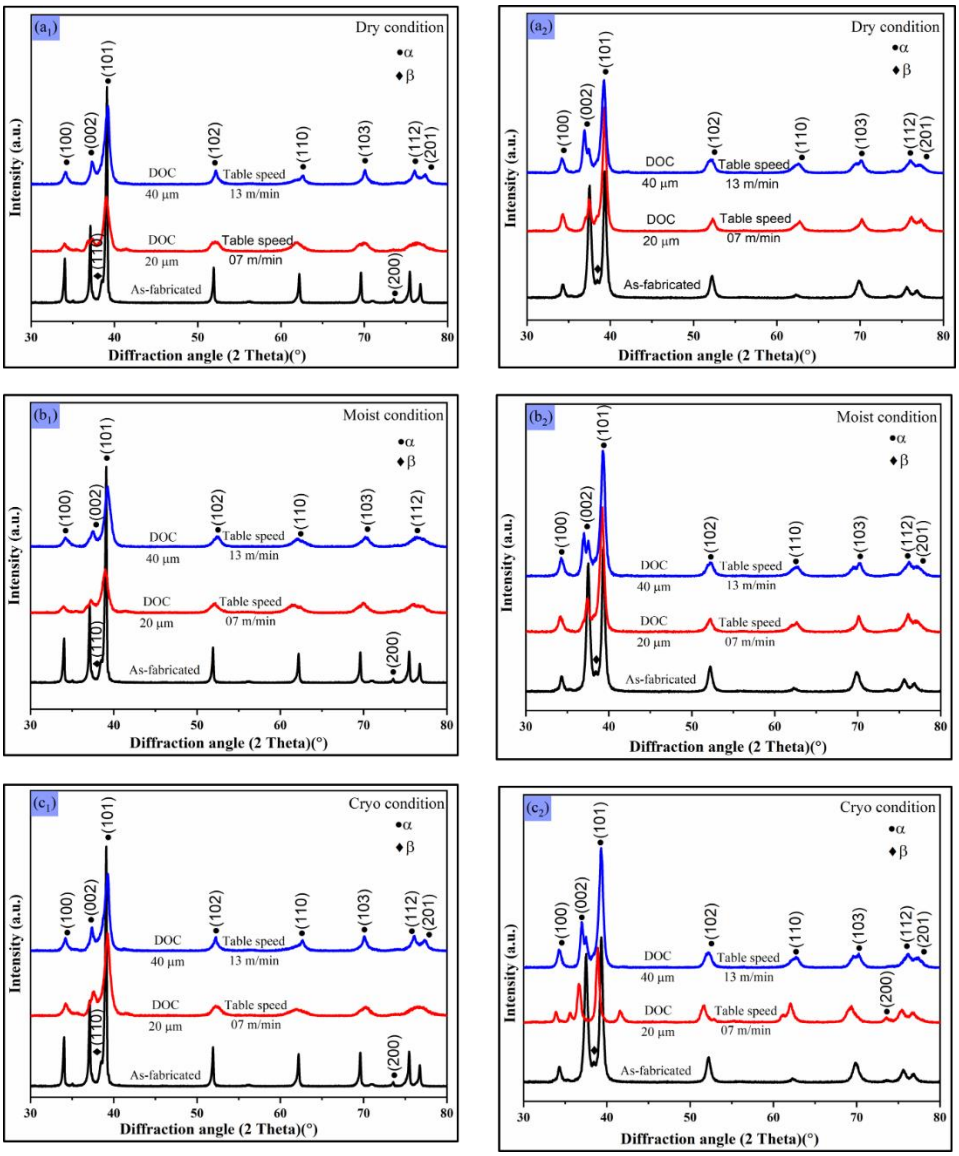

Figure 4.14 XRD patterns at DOC of 40, 20 µm and table feeds of 07, 13 m/min for various grinding conditions: (a) dry, (b) moist, and (c) cryogenic conditions. Subscript 1 is for AM and 2 for conventionally manufactured samples

4.1.12 Effect of grinding media on subsurface layer of the finished AM and conventionally manufactured samples

Figure 4.15 and Figure 4.16 present the effect of various grinding conditions on the subsurface layers of finished additively manufactured and conventionally manufactured samples, respectively. The finishing process introduced heat and altered the microstructure, depending on the grinding conditions. To identify the effect of finishing process on microstructural change within the affected layer of the samples, the microstructure of each finished Ti-6Al-4V sample after dry, moist and cryogenic finishing are shown in Figure 4.15 and Figure 4.16 respectively.

From these figures, it is clear that grain refinement occurred on the finished surface in all the environment conditions. The subsurface region shows a significant difference in microstructure from grinding in different environmental conditions [196]. The additively manufactured Ti-6Al-4V sample is known to have a fine martensitic microstructure due to the rapid solidification from fast cooling during the process. After heat treatment, the material is having α and β phases.

Grinding the surface may also alter the microstructure in the subsurface layer since the material is having a mixture of α and β phases [106]. In the subsurface layers, just below the finished surface (~20 μm), smaller α grains were observed and β grains were almost diminished, as shown in Figure 4.15 and Figure 4.16. The smallest grains were observed under cryogenic finishing conditions, compared to dry and moist finishing as also observed earlier [203]. It shows how cryogenic cooling prevents grain growth at lower grinding temperatures. It also supports the potential of using cryogenic cooling to produce harder and stronger finished surface in comparison to dry and moist finishing.

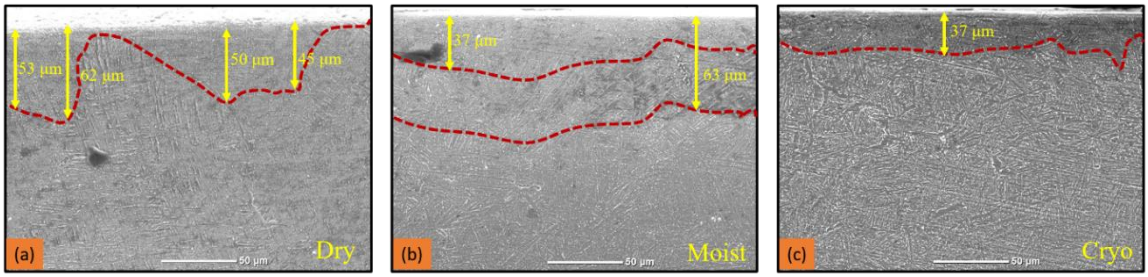

Figure 4.15 SEM micrographs of subsurface layers of finished AM samples in (a) dry, (b) wet, and (c) cryo conditions

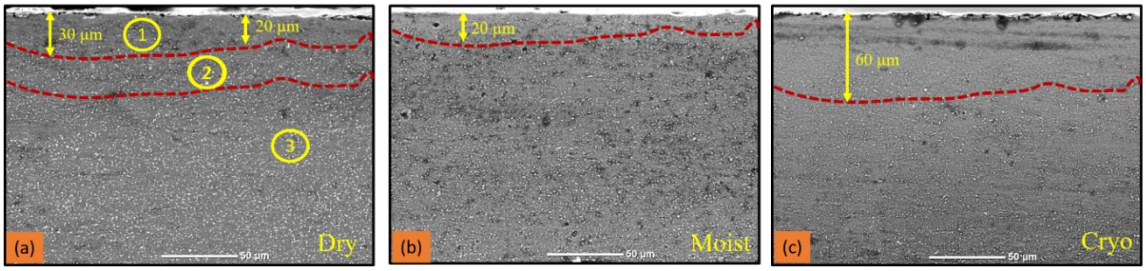

Figure 4.16 SEM micrographs of subsurface layers of finished conventional samples in (a) dry, (b) wet, and (c) cryo conditions

4.1.13 Grinding chip morphology

Figure 4.17 represents the microstructure of microchips resulting from grindings in various grinding environments. Microchips generated during the grinding process provide information about the performance of the coolant. These microchips are formed by the ploughing and shearing action of the abrasive grits of the grinding wheel on the surface of the workpiece. Un-melted powder particles were observed in microchips in all the grinding conditions. Smooth frontal and rough backside of microchips were observed, as shown in Figure 4.17 (b), (d), and (f). The maximum heat generated in dry grinding is crucial to regulate the formation of various types of microchips.

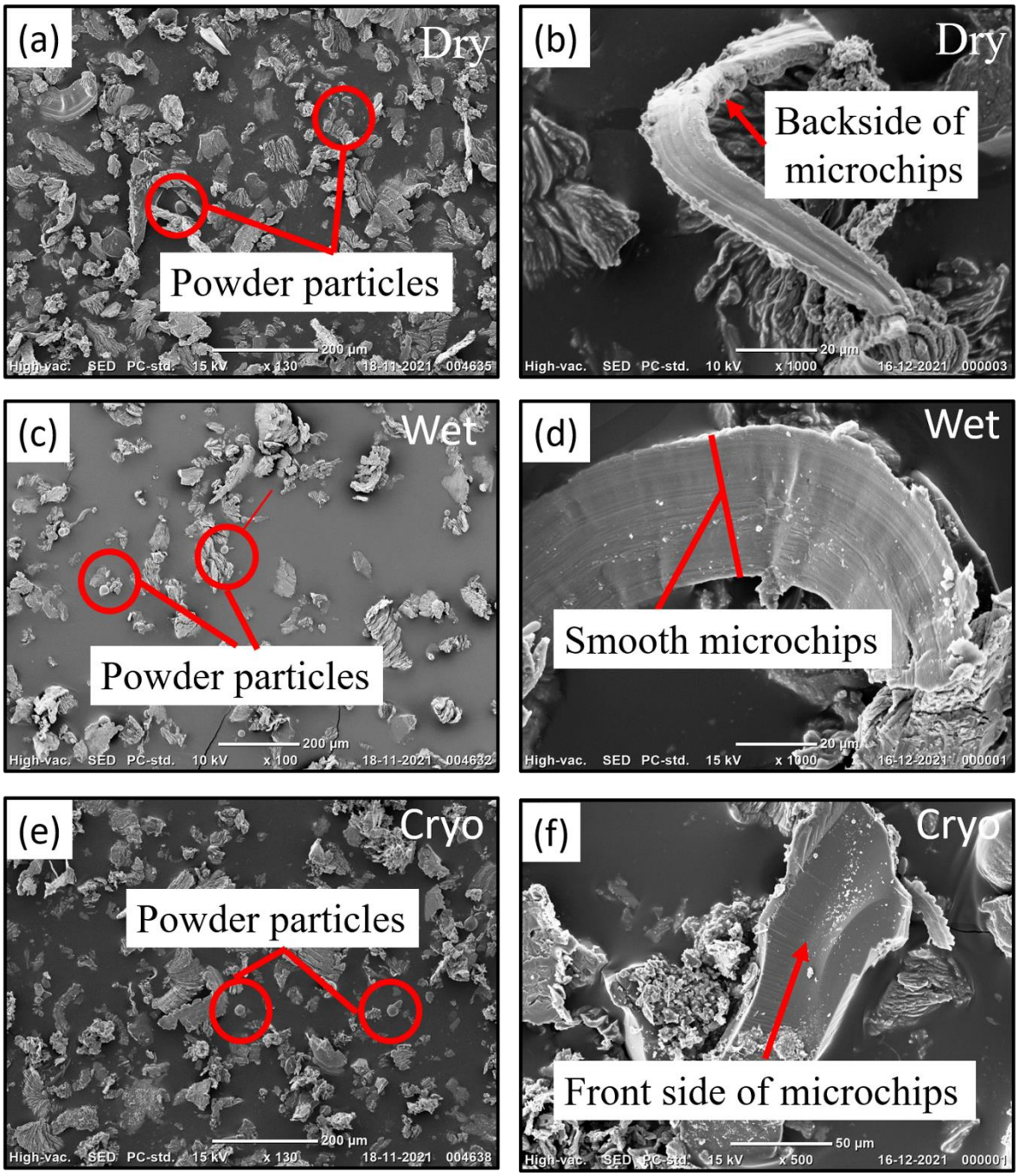

Figure 4.17 Microstructure of microchips: (a, b) dry, (c, d) wet, and (d, e) cryogenic conditions

Due to this, a large number of globular and thicker microchips were identified, as mentioned in Figure 4.17 (a). The main reason for the formation of thicker microchips is due to large action of shearing and ploughing of abrasive grits on work material [204]. Additionally, in the absence of coolant during dry grinding, heat is accumulated near the

grinding region, and due to this, large microchips are converted into small globules [205]. During wet grinding, the coolant was used and that carried out the heat generated from the grinding region, providing sufficient cooling during grinding. The un-melted powder particles were also observed in wet grinding, as shown in Figure 4.17 (c) and (e). Some wear tracks were also observed because of the formation of the hydrodynamic boundary layer during wet grinding. Due to a reduction in ploughing action during cryogenic grinding, thin with no wear tracks microchips were observed as shown in Figure 4.17 (f).

4.1.14 Optimization with regression modelling

During grinding of L-PBF Ti-6Al-4V components at different depth of cuts and table speeds under different grinding conditions, the regression model was carried out to get the output responses using Minitab software (version 19). Table 4.1 demonstrates the input variables and their levels utilized to optimize the parameters.

Table 4.1 Grinding input variables and their levels

S No.	Input variables	Levels		
		Low (-1)	**Medium (0)**	**High (1)**
1	**Depth of cut, DOC (µm)**	10	20	30
2	**Table speed, V_t (m/min)**	7	10	13
3	**Environment**	Dry	Wet	Cryo

The regression model considered the most essential terms (eliminated the insignificant terms of third order of individual input parameters) that affect the output responses under different grinding environment conditions and same are illustrated below:

For dry grinding condition:

$$Surface\ roughness\ (\mu m) = 0.087 + 0.0001\ DOC + 0.0504\ V_t + 0.000015\ DOC * DOC - 0.00267\ V_t * V_t + 0.000592\ DOC * V_t \quad \text{..... (4.1)}$$

$$Tangential\ force\ (N) = 44.8 - 1.000\ DOC - 8.50\ V_t + 0.389\ V_t * V_t + 0.1667\ DOC * V_t \quad \text{...(4.2)}$$

For wet grinding condition:

$$Surface\ roughness\ (\mu m) = 0.3150 + 0.001750\ DOC + 0.00041\ V_t - 0.000033\ DOC * DOC + 0.000019\ V_t * V_t + 0.000058\ DOC * V_t \quad \text{... (4.3)}$$

$$Tangential\ force\ (N) = 41.0 - 1.917\ DOC - 5.85\ V_t + 0.0283\ DOC * DOC + 0.259\ V_t * V_t + 0.1333\ DOC * V_t \quad \text{... (4.4)}$$

For cryogenic grinding condition:

$$Surface\ roughness\ (\mu m) = 0.098 + 0.00037\ DOC + 0.0226\ V_t - 0.000053\ DOC * DOC - 0.00109\ V_t * V_t + 0.000683\ DOC * V_t \quad \text{... (4.5)}$$

$$Tangential\ force\ (N) = 6.59 - 0.367\ DOC - 0.35\ V_t + 0.00833\ DOC * DOC + 0.0370\ V_t * V_t + 0.0250\ DOC * V_t \quad \text{... (4.6)}$$

Here, DOC is depth of cut (µm) and V_t is table speed (m/min).

The created model for R_a value and tangential forces was obtained with R_{sq} value of 91.19% and 97.6% for dry, 99.5% and 98.43% for wet, and 95.97% and 95.49% for cryogenic conditions respectively. The acceptability of obtained regression model is verified at a depth of cut of 10 µm and table speed of 7 m/min. The percentage error was calculated between the experimental value and regression model and is mentioned in

Table 4.2. The third order of individual input parameters were eliminated in the model due to insignificant variables. A maximum deviation of 12.5% and 17.08% was observed for the surface roughness and tangential force between experimental value and regression model under dry environment as shown in Table 4.2. For other grinding conditions, the deviations are much lower, which confirms the acceptability of the developed regression model.

Table 4.2 Percentage error of regression model from the experimental value

Output parameters	**Experimental value**			**Regression model**			**Error (%)**		
	Dry	**Wet**	**Cryo**	**Dry**	**Wet**	**Cryo**	**Dry**	**Wet**	**Cryo**
Surface roughness (µm)	0.356	0.337	0.259	0.31147	0.337061	0.249	12.5	0.018	3.86
Tangential force (N)	5	5	5	6.03	5.732	4.866	17.08	12.77	2.68

With the above results and discussion of surface characteristics of AM fabricated Ti-6Al-4V alloy, results and discussion of corrosion behaviour of AM fabricated Ti-6Al-4V alloy has been discussed in chapter 5.